MOLECULAR AND CELLULAR BIOLOGY, Jan. 2008, p. 237–247 Vol. 28, No. 1
0270-7306/08/$08.00+0 doi:10.1128/MCB.01065-07

Apoptosis-Inducing Factor Is a Target for Ubiquitination through Interaction with XIAP▽†

John C. Wilkinson,[1]‡ Amanda S. Wilkinson,[1]‡ Stefanie Galbán,[1] Rebecca A. Csomos,[1] and Colin S. Duckett[1,2]*

Departments of Pathology[1] and Internal Medicine,[2] University of Michigan, Ann Arbor, Michigan 48109

Received 15 June 2007/Returned for modification 19 July 2007/Accepted 8 October 2007

X-linked inhibitor of apoptosis (XIAP) is an inhibitor of apoptotic cell death that protects cells by caspase-dependent and independent mechanisms. In a screen for molecules that participate with XIAP in regulating cellular activities, we identified apoptosis-inducing factor (AIF) as an XIAP binding protein. Baculoviral IAP repeat 2 of XIAP is sufficient for the XIAP/AIF interaction, which is disrupted by Smac/DIABLO. In healthy cells, mature human AIF lacks only the first 54 amino acids, differing significantly from the apoptotic form, which lacks the first 102 amino-terminal residues. Fluorescence complementation and immunoprecipitation experiments revealed that XIAP interacts with both AIF forms. AIF was found to be a target of XIAP-mediated ubiquitination under both normal and apoptotic conditions, and an E3 ubiquitin ligase-deficient XIAP variant displayed a more robust interaction with AIF. Expression of either XIAP or AIF attenuated both basal and antimycin A-stimulated levels of reactive oxygen species (ROS), and when XIAP and AIF were expressed in combination, a cumulative decrease in ROS was observed. These results identify AIF as a new XIAP binding partner and indicate a role for XIAP in regulating cellular ROS.

Apoptosis is a cellular death program critical to the development and homeostatic maintenance of all multicellular organisms (27, 39), and deregulated apoptosis has been implicated in many disease states (52). The principal biochemical mediators of apoptosis are caspases, cysteinyl proteases that are activated in a precisely orchestrated manner following various death triggers (12, 53). Apoptotic caspases are divided into two groups: initiator caspases, which respond to and are directly activated by apoptotic stimuli, and effector caspases, which carry out completion of the apoptotic program (3, 40).

Predominant among the molecules that play a role in controlling caspase activity are members of the inhibitor of apoptosis (IAP) family (13, 21). Among the eight mammalian IAP homologues that have been described, X-linked inhibitor of apoptosis (XIAP) (15, 32, 54) has emerged as the most potent suppressor of apoptosis. XIAP binds and inhibits the initiator caspase 9 (47, 50) and the effector caspases 3 (23, 44) and 7 (8) and can thus regulate multiple steps within the caspase cascade. While many IAP proteins can attenuate cell death, XIAP appears to be the only IAP homologue to directly inhibit caspases with high affinity (16).

Distinct patterns of caspase activation exist, and so far two major apoptotic pathways have been described. Ligation of members of the tumor necrosis factor receptor family activates an extrinsic death program by forming an intracellular death-inducing signaling complex (DISC) (35). The DISC recruits and activates initiator caspases, such as caspases 8 and 10, which in turn engage downstream effector caspases. In contrast, death signals such as cellular stress induce an intrinsic apoptotic program regulated predominantly by the mitochondria. These stimuli induce mitochondrial outer membrane permeabilization, thus allowing the cytoplasmic release of pro-apoptotic molecules sequestered within the mitochondria. Notable among these sequestered factors are cytochrome *c*, which along with the adaptor molecule Apaf-1 (31) forms an oligomeric complex known as the apoptosome (6) leading to caspase 9 activation. Additional factors include Smac/DIABLO (14, 58) and Omi/HtrA2 (19, 34, 59), which promote apoptosis in part by neutralizing XIAP-mediated caspase inhibition (7, 33, 48), and the flavoprotein apoptosis-inducing factor (AIF).

While cytochrome *c*, Smac/DIABLO, and Omi/HtrA2 promote cell death predominantly by caspase-dependent mechanisms, AIF was originally described as a caspase-independent mediator of cell death (51). Mitochondrial release of AIF ultimately results in AIF nuclear translocation and DNA binding (63) and is associated with chromatin condensation and internucleosomal DNA cleavage. Interestingly, AIF possesses NADH oxidase activity in vitro (36), and recent studies have described a protective role for AIF, in part through maintaining the expression and activity of complex I of the electron transport chain (55). Further studies in vivo have suggested a protective role for AIF against certain forms of oxidative stress (28), and loss of AIF in heart and brain results in severe defects, most likely caused by loss of mitochondrial integrity (9, 26).

Like AIF, XIAP is involved in several pathways both related to and distinct from apoptosis. Through interactions with members of the transforming growth factor β receptor family, XIAP regulates Smad-dependent transcriptional activation (2, 25, 61). Ectopic XIAP expression regulates stress-responsive

* Corresponding author. Mailing address: BSRB, Room 2057, 109 Zina Pitcher Place, Ann Arbor, MI 48109-2200. Phone: (734) 615-6414. Fax: (734) 763-2162. E-mail: colind@umich.edu.

† Supplemental material for this article may be found at http://mcb.asm.org/.

‡ Present address: Department of Biochemistry, Wake Forest University School of Medicine, Medical Center Boulevard, Winston-Salem, NC 27157.

▽ Published ahead of print on 29 October 2007.

pathways, including those involving N-terminal c-Jun kinase (JNK) (45, 46) and the transcription factor NF-κB (20, 29). Interestingly, the ability of XIAP to regulate these pathways can be uncoupled from its caspase-inhibitory activities (30), suggesting that these are distinct properties of the protein. XIAP also controls intracellular copper levels, both through ubiquitin ligase-dependent regulation of the copper binding protein COMMD1 (4) and by binding copper directly (37). In light of the fact that XIAP-deficient mice display no overt apoptotic phenotype (18), these findings suggest that in most normal tissues the primary function(s) of XIAP may be to regulate pathways distinct from those involving apoptotic caspase cascades. This is similar to many apoptotic regulators, such as cytochrome *c* and Bad, which under normal conditions participate in processes other than cell death regulation (17, 43).

To explore the possibility that XIAP regulates biological processes beyond those described above, we conducted a biochemical screen for XIAP-associated proteins and identified AIF as an XIAP binding protein. XIAP binds both the mature form of AIF present in healthy cells and the processed form of AIF released from mitochondria during apoptosis (41). The XIAP/AIF interaction depends on the presence of the second baculoviral IAP repeat (BIR) domain of XIAP and can be specifically displaced by Smac/DIABLO. Unlike that of XIAP antagonists, AIF overexpression fails to prevent XIAP-mediated caspase activation. Under both normal and apoptotic conditions XIAP induces AIF ubiquitination in a manner that does not result in degradation but instead appears to affect the stability of the XIAP/AIF interaction. Finally, XIAP and AIF combine to attenuate levels of both basal and antimycin A-stimulated reactive oxygen species (ROS). Taken together, these data define a novel interaction between two well-known regulators of the cell death pathway and provide the foundation for uncovering new mechanisms by which XIAP and AIF regulate both apoptotic and nonapoptotic cellular processes.

MATERIALS AND METHODS

Materials. Reagents were obtained as follows: protein G-coupled agarose, Ni-nitrilotriacetic acid (NTA) agarose, Glutamax, tobacco etch virus protease, Mitotracker Red, and phosphate-buffered saline from Invitrogen; glutathione-Sepharose 4B, calmodulin-Sepharose 4B, and immunoglobulin G (IgG)-Sepharose from Amersham; fetal bovine serum from HyClone; Dulbecco modified Eagle medium (DMEM) from Mediatech; ApoTarget protease assay kit from Biosource; DEVD–7-amino-4-trifluoromethyl coumarin from BioMol; site-directed mutagenesis kit from Stratagene; and protease inhibitor tablets from Roche. All other chemicals were from Sigma. Antibodies were obtained as follows: anti-XIAP and anti-AIF from BD-Pharmingen; anti-AIF from Santa Cruz Biotechnology; cleaved caspase 3 from Cell Signaling; anti-Smac/DIABLO from Calbiochem; anti-glutathione *S*-transferase (anti-GST) from Santa Cruz Biotechnology; anti-β-actin, horseradish peroxidase (HRP)-conjugated anti-FLAG, and HRP-conjugated antihemagglutinin (anti-HA) from Sigma; and HRP-conjugated anti-mouse and anti-rabbit antibodies from Amersham.

Cell culture, transfections, and plasmids. HEK 293 cells were grown in DMEM containing 10% fetal bovine serum supplemented with 2 mM Glutamax at 37°C in an atmosphere of 95% air and 5% CO_2. Transfections were performed by the method of calcium phosphate precipitation as described previously (15). pEBB XIAP-TAP and pEBB D148A/W310A XIAP-TAP were generated by subcloning wild-type (WT) and D148A/W310A XIAP into the pEBB tandem affinity purification (TAP) plasmid. The bimolecular fluorescence complementation (BiFC) plasmids pEBB YN and pEBB YC were generated by PCR using pBIFC-YN155 and pBIFC-YC155 (gifts of T. Kerppola, University of Michigan) as templates, respectively. pEBB YN-XIAP was generated by subcloning WT XIAP into pEBB-YN. pEBB AIF was generated by PCR using an expressed sequence tag clone containing full-length human AIF (Image clone 5740894) and was used to further subclone pEBB AIF-TAP, pEBB AIF-YFP, pEBB AIF-FLAG, and pEBB AIF-YC. pEBB Ub-Smac/DIABLO A1G and pEBB Ub-Smac/DIABLO ΔA1 were generated by site-directed mutagenesis (Stratagene) using pEBB Ub-Smac/DIABLO as template. pEBB Ub-Δ54AIF-FLAG and pEBB Ub-Δ102AIF-FLAG were generated by PCR using pEBB-AIF-FLAG as template followed by replacement of the Smac/DIABLO sequence within the pEBB Ub-Smac/DIABLO-FLAG construct. These plasmids were then used as templates for PCR amplification in the subcloning of pEBB Ub-Δ54AIF, pEBB Ub-Δ102AIF, pEBB Ub-Δ102AIF-YFP, and pEBB Ub-Δ102AIF-YC. All remaining plasmids used in this study have been reported previously (4, 5, 60).

TAP. Cells were seeded into a total of 10 15-cm plates and then transfected with 12 μg of pEBB XIAP-TAP or pEBB D148A/W310A XIAP-TAP per plate. Two days after transfection, the cells were harvested, lysed, and subjected to TAP as described previously (5). Final purified samples were submitted to the Proteomics Centre at the University of Victoria for further processing including trypsin digestion, high-pressure liquid chromatography separation, and tandem mass spectrometry to determine peptide sequences.

Cell lysis, Coomassie blue staining, immunoblot analysis, and immunoprecipitation. Cell lysates were prepared in either RIPA buffer (phosphate-buffered saline containing 1% NP-40, 0.5% sodium deoxycholate, 0.1% sodium dodecyl sulfate [SDS]) or Triton lysis buffer (25 mM HEPES, pH 7.9, 100 mM NaCl, 1% Triton X-100, 1 mM EDTA, 10% glycerol, 1 mM NaF, 1 mM $NaVO_4$) (both lysis buffers were supplemented with 1 mM dithiothreitol, 1 mM phenylmethylsulfonyl fluoride, and 1 protease inhibitor cocktail tablet per 10 ml prior to use), normalized for protein content, and then separated by SDS-polyacrylamide gel electrophoresis (PAGE) using 4 to 12% gradient SDS-polyacrylamide gels (Invitrogen). Coomassie blue staining was performed using the Colloidal Blue staining kit (Invitrogen) according to the manufacturer's instructions. For immunoblot analysis, SDS-PAGE was followed by transfer to nitrocellulose membranes (Invitrogen), which were then blocked with 5% milk in Tris-buffered saline containing 0.02 to 0.2% Tween, followed by incubation with the indicated antibodies for 1 h at room temperature. Following washing, membranes were incubated with HRP-conjugated anti-mouse IgG or anti-rabbit IgG secondary antibodies for 45 min at room temperature and visualized by enhanced chemiluminescence. For immunoprecipitation experiments, cell lysates (Triton lysis buffer) were normalized for protein content and incubated with indicated antibodies for 2 h at 4°C. Protein G-coupled agarose beads were then added and incubated for 1 h. For precipitation of GST-tagged proteins or His_6-ubiquitin-conjugated proteins, glutathione-Sepharose beads or nickel agarose beads were added and the samples were incubated at 4°C for 2 h. Agarose beads were recovered by centrifugation and washed in Triton buffer, and precipitated proteins were eluted by adding lithium dodecyl sulfate sample buffer and heating the mixture to 95°C for 5 min. Recovered proteins were then separated by electrophoresis, and immunoblot analysis was carried out as described above.

Amino-terminal protein sequencing. Cells were seeded in five 15-cm plates and transfected with 12 μg each of pEBB AIF-TAP. After 2 days, cell lysates were subjected to TAP as described above, except that the final eluate was collected as a single fraction and was not precipitated with trichloroacetic acid. A portion of the eluate was analyzed by colloidal Coomassie blue staining as described above. The remaining sample was then submitted to the Proteomics Centre at the University of Victoria for further processing, including separation by SDS-PAGE, transfer to polyvinylidene difluoride (PVDF), and amino-terminal protein sequencing by Edman degradation.

Fluorescence microscopy/BiFC. Cells were seeded on polylysine-coated chambered coverglass slides and then transfected as follows: for plasmids encoding yellow fluorescent protein (YFP) fusion proteins, a total of 2 μg of each plasmid was used per well; for BiFC plasmids, 1 μg of each plasmid encoding a BiFC fusion protein (YN or YC, 2 μg total DNA) was used per well. Twenty-four hours after transfection, medium was replaced with phenol red-free DMEM and cells were incubated for an additional 24 h. Cells were then stained with Hoechst 33342 and Mitotracker Red (Molecular Probes/Invitrogen) and examined using a Zeiss Axiovert 100 M confocal microscope equipped with a Zeiss LSM 510 spectrometer.

Caspase activity assay. Cells were seeded in six-well plates; transfected 24 h later with pEBB-GFP, pCDNA3-Bax, and other plasmids; and then incubated at 37°C for 16 h. Floating and attached cells were harvested, and caspase 3 assays were performed as described previously (60).

Measurement of intracellular ROS levels. Cells were seeded in six-well plates and transfected by calcium phosphate. After 48 h cells were left untreated or treated with 10 μg/ml antimycin A for 1 hour at 37°C. Following treatment cells were incubated with the ROS indicator dye CM-H_2DCF-DA (Molecular Probes/Invitrogen) for an additional 30 min at 37°C. Cells were then harvested by

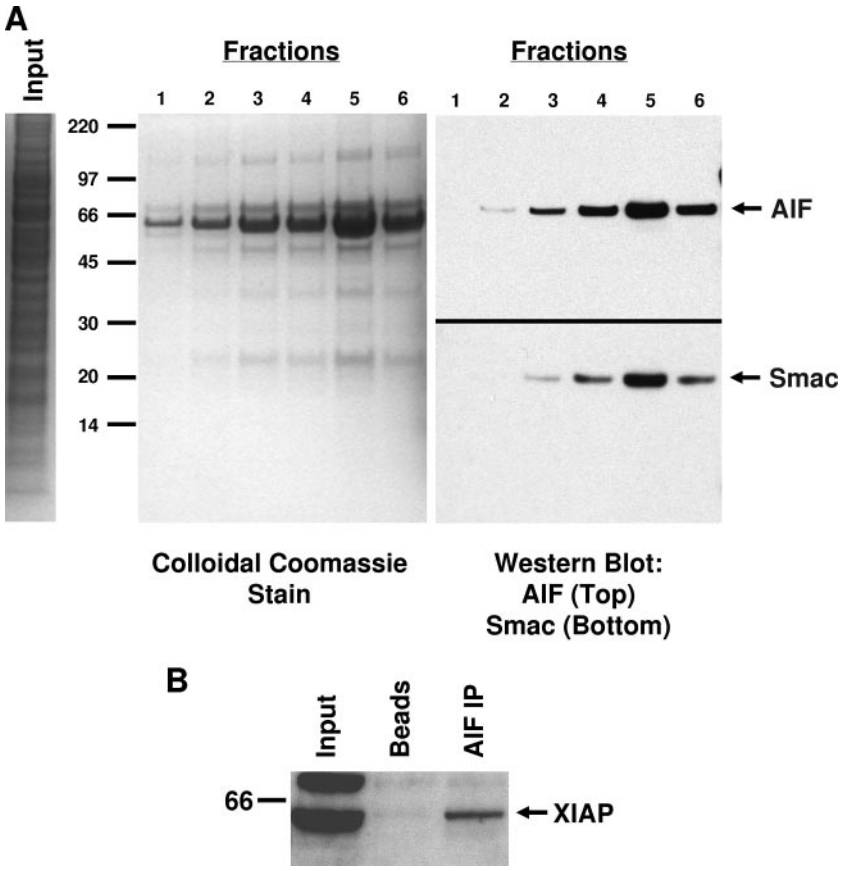

FIG. 1. AIF is an XIAP-associated factor. (A) D148A/W310A XIAP-TAP was expressed in HEK 293 cells. A cell lysate was prepared and subjected to TAP. Total protein in input and final eluted fractions was visualized by SDS-PAGE and Coomassie blue staining (left and middle panels), showing XIAP bait protein and associated factors. Eluted fractions were pooled, precipitated with trichloroacetic acid, and digested with trypsin, and peptides were identified by mass spectrometry. Eluted fractions were also immunoblotted for the presence of AIF and Smac (right panel). (B) Untransfected HEK 293 cell lysate was precipitated with either beads alone or beads bound to an AIF-specific antibody, and the presence of XIAP in precipitated complexes was assessed by immunoblot analysis. Numbers at left of the panels are molecular masses in kilodaltons.

trypsinization and analyzed using either a Beckman-Coulter Cytomics FC 500 or a Becton Dickinson FACSCalibur flow cytometer.

RESULTS

To identify factors that participate with XIAP in regulating caspase-independent processes, a biochemical screen for XIAP-associated proteins was performed using the TAP method (42). This screen employed as bait the XIAP variant D148A/W310A, which fails to inhibit caspases 3, 7, and 9 (30), in fusion with a carboxy-terminal TAP tag, which was chosen in order to avoid masking potential interaction partners due to XIAP/caspase interactions. Coomassie blue staining of purification eluates showed a significant amount of bait material, as well as a number of additional bands of both higher and lower molecular weights (Fig. 1A, left panel). Purified material was precipitated by trichloroacetic acid and digested with trypsin, and potential XIAP-interacting proteins were identified by liquid chromatography-tandem mass spectrometry analysis of generated peptides. This approach identified a number of novel XIAP-associated proteins (see Table S1 in the supplemental material), including the mitochondrial flavoprotein AIF. The presence of AIF in eluted fractions was confirmed by immunoblot analysis, using Smac/DIABLO as a control (Fig. 1A, right panel). Given the roles that both XIAP and AIF play in regulating apoptotic and nonapoptotic processes, this interaction represents a potentially novel finding for cellular regulation and became the focus for further characterization. The ability of XIAP and AIF to coassociate was confirmed with endogenous proteins by immunoprecipitation analysis. AIF was precipitated from HEK 293 cells, and the presence of XIAP was assessed by immunoblot analysis. As shown in Fig. 1B, XIAP was readily detected in AIF immune complexes, confirming the association between endogenous XIAP and AIF.

The structural determinants within XIAP that are required for binding to AIF were next assessed. XIAP contains three amino-terminal BIR domains followed by a RING domain at the carboxy terminus. Plasmids encoding XIAP domains in fusion with GST were transfected into HEK 293 cells along with a plasmid encoding full-length human AIF with a FLAG tag at the carboxy terminus. Cellular lysates were then precipitated with glutathione beads, and the presence of AIF in

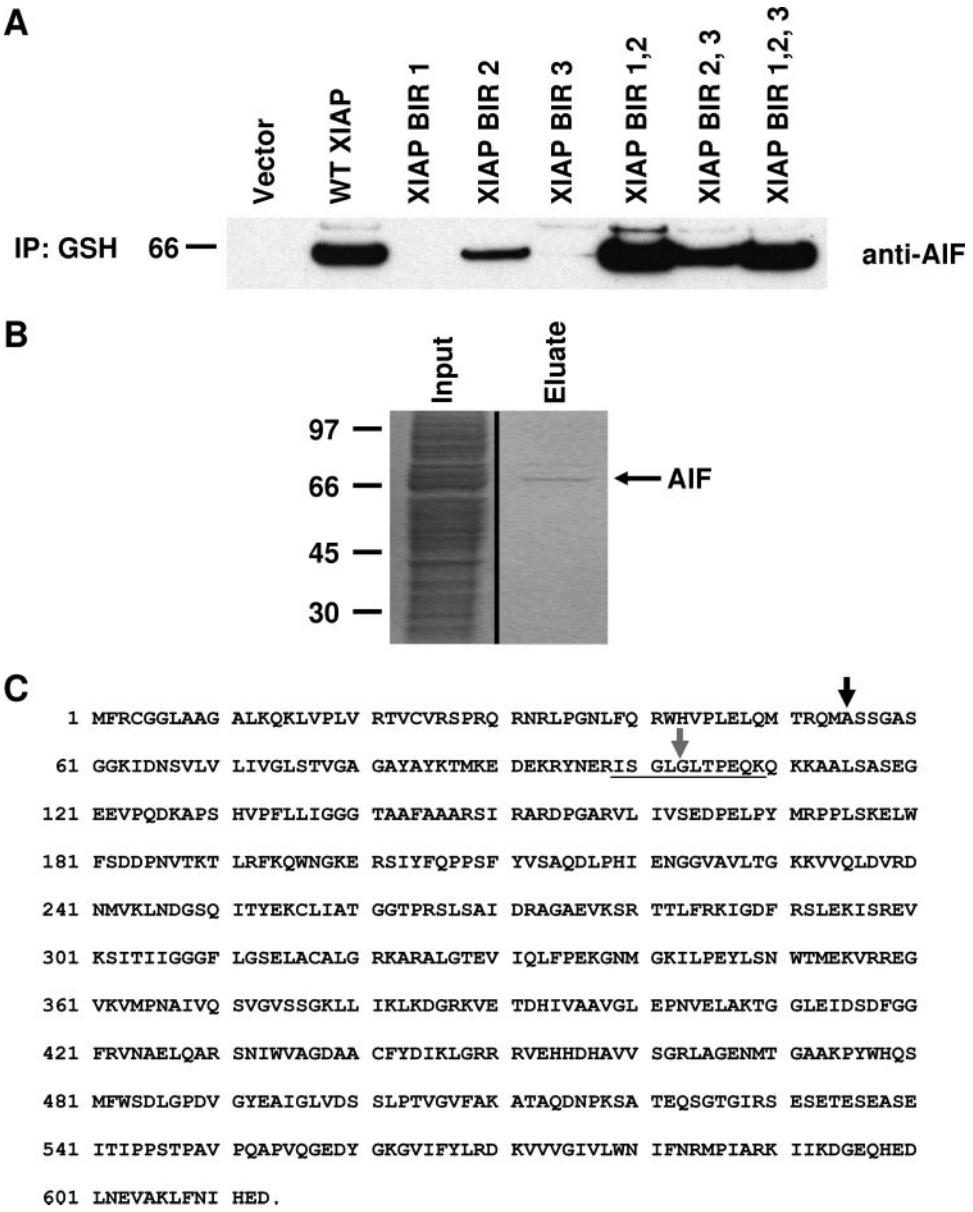

FIG. 2. BIR2 of XIAP binds AIF; mature AIF begins at residue 55. (A) HEK 293 cells were transfected with plasmids encoding various XIAP domain truncations in fusion with GST along with a plasmid encoding full-length human AIF. Cell lysates were prepared, and XIAP was precipitated with glutathione (GSH) beads. The presence of AIF in precipitated complexes was determined by immunoblotting. (B) Full-length human AIF-TAP was expressed in HEK 293 cells. AIF was precipitated from cell lysates using IgG-Sepharose beads; eluted proteins were then separated by SDS-PAGE and transferred to PVDF membranes. Following Coomassie blue staining, the AIF band was excised and subjected to Edman degradation in order to determine the mature amino terminus. Numbers at left of panels A and B are molecular masses in kilodaltons. (C) Primary sequence of full-length human AIF. The underlined sequence is one of four AIF peptides recovered from analysis of XIAP-TAP. The gray arrow is the first residue of mature AIF as reported by reference 51; the black arrow is the first residue of mature human AIF as determined by this study.

precipitated complexes was assessed by immunoblot analysis. As shown in Fig. 2A, XIAP BIR2 was found to be sufficient to precipitate AIF, indicating that this region is critical for AIF association.

AIF undergoes amino-terminal processing to generate the mature form, originally reported to begin at residue 102 in the mouse protein (residue 103 in human) (51). When examining the peptides recovered from the XIAP-TAP screen, we observed that one AIF-specific peptide spanned the region surrounding residue 103 (Fig. 2C), raising the possibility that mature AIF begins at a position farther upstream than originally reported. To test this possibility, full-length human AIF in fusion with a carboxy-terminal TAP tag was expressed in HEK 293 cells. TAP-tagged AIF then was recovered from cell lysates by TAP, subjected to SDS-PAGE, transferred to a PVDF membrane, and visualized by Coomassie blue staining (Fig. 2B). The band corresponding to AIF was excised, and Edman degradation was performed to determine the mature

amino terminus. These results indicated that the mature terminus of human AIF begins at residue 55, rather than the residue originally reported (Fig. 2C). This observation is in agreement with a recent study characterizing the processing of rat AIF expressed in HeLa cells (41), which indicated that AIF exists in two forms within cells: a mature, nonapoptotic form truncated to position 54 (residue 55 in the human protein) and an apoptotic form truncated to position 102 (residue 103 in the human protein).

Like AIF, the XIAP antagonist Smac/DIABLO undergoes proteolytic processing to generate a mature amino terminus, which contains a canonical IAP binding motif (IBM). IBMs have a strong preference for an alanine residue in the first position, and alteration of this alanine is often sufficient to prevent IAP binding (57). Neither the healthy nor the apoptotic forms of AIF appear to contain a consensus IBM sequence, though this possibility could not be ruled out. Thus, to compare the abilities of both the healthy and mature forms of AIF to interact with XIAP, two different AIF encoding strategies were used. In the first approach, cDNAs encoding either the Δ54 or the Δ102 form of AIF were expressed following a single start codon (met-Δ54AIF and met-Δ102AIF, respectively [Fig. 3A]). However, this approach results in the incorporation of a methionine residue at the amino terminus of each protein that could potentially interfere with binding to XIAP. We therefore chose an alternative strategy in which each AIF variant was expressed in fusion with a ubiquitin polypeptide at the amino terminus (24). Ubiquitin undergoes cotranslational processing, resulting in a proteolytic event at the extreme carboxy-terminal diglycine of ubiquitin. This event releases ubiquitin and leaves the amino terminus of AIF free of any additional residues. Therefore, we generated Ub-Δ54AIF and Ub-Δ102AIF fusion polypeptides, which undergo processing into the healthy and apoptotic AIF forms, respectively (Fig. 3A).

The panel of AIF variants was then tested for interaction with XIAP. As shown in Fig. 3A, XIAP efficiently precipitated all forms of AIF except Ub-Δ102AIF. The ability of XIAP to bind both met-Δ54AIF and met-Δ102AIF confirms the lack of an IBM at the amino terminus of AIF and suggests that AIF binds XIAP through a non-IBM motif. When input material was immunoblotted for AIF, a pattern of laddering consistent with ubiquitination was observed for the full-length, Ub-Δ54AIF, and Ub-Δ102AIF variants and was noticeably absent for both the met-Δ54 and met-Δ102 forms. Since met-Δ102AIF protein bound XIAP efficiently, in contrast to the Ub-Δ102AIF form, which failed to bind but displayed the greatest extent of laddering, these data raised the possibility that AIF may be a target for ubiquitination, which may in turn regulate stability of the XIAP/AIF complex.

XIAP possesses E3 ubiquitin ligase activity, a property that is conferred by the RING domain at the carboxy terminus (62). The data presented above suggested that AIF is ubiquitinated and may thus be a substrate for the E3 ligase activity of XIAP. To test this possibility, cells were transfected with plasmids encoding His-tagged ubiquitin and either full-length AIF, Ub-Δ54AIF, or Ub-Δ102AIF in the absence and presence of XIAP. Ni-NTA beads were then used to precipitate ubiquitinated proteins from cell lysates, and the presence of AIF in these complexes was determined by immunoblotting (Fig. 3B).

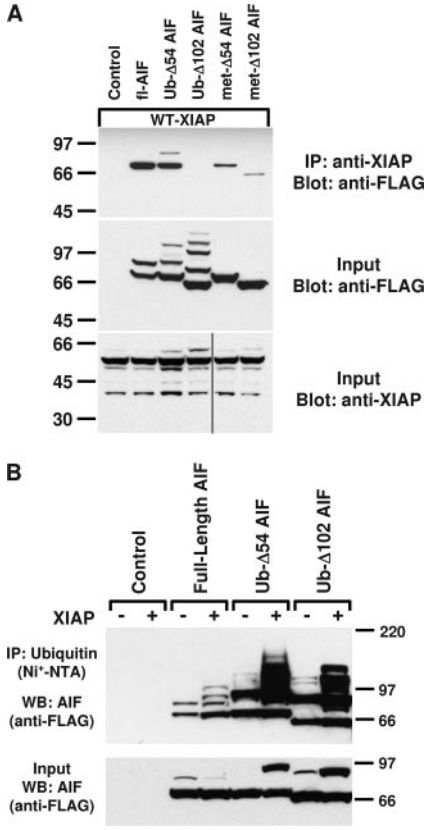

FIG. 3. XIAP binds AIF variants and mediates AIF ubiquitination. (A) HEK 293 cells were transfected with a plasmid encoding WT-XIAP along with control, full-length AIF, Ub-Δ54AIF, Ub-Δ102AIF, met-Δ54AIF, or met-Δ102AIF expression plasmids. Cell lysates were then prepared and precipitated with anti-XIAP. The presence of AIF in precipitated complexes was determined by immunoblot analysis for the FLAG tag present at the carboxy terminus of each AIF protein (top panel). Equivalent expression of XIAP and AIF variants was confirmed by immunoblotting input lysates with anti-FLAG (middle panel) or anti-XIAP (bottom panel). The black line present in the bottom panel indicates removal of a single empty lane solely for the purpose of clarity. (B) HEK 293 cells were transiently transfected with His-tagged ubiquitin and plasmids expressing full-length AIF-FLAG, Ub-Δ54AIF-FLAG, and Ub-Δ102AIF-FLAG in the absence and presence of an XIAP expression plasmid. Ubiquitinated material was then precipitated using Ni-NTA beads, and the presence of FLAG-tagged proteins (AIF) in precipitated complexes was detected by immunoblot analysis. Numbers at left of panel A and at right of panel B are molecular masses in kilodaltons.

All three AIF variants displayed significant basal ubiquitination in the absence of overexpressed XIAP, possibly due to either endogenous XIAP or alternative E3 ligases. Upon XIAP overexpression the amount of ubiquitinated material recovered for all three forms of AIF, including Ub-Δ102AIF, increased substantially above basal levels. These data suggest that both the healthy and apoptotic forms of AIF are targets for XIAP-mediated ubiquitination. Interestingly, AIF ubiquitination by XIAP did not result in degradation (as shown by AIF input levels), suggesting that this process does not target AIF to the proteasome and raising the possibility that ubiquitination of AIF by XIAP may instead alter the enzymatic or death-inducing properties of the molecule.

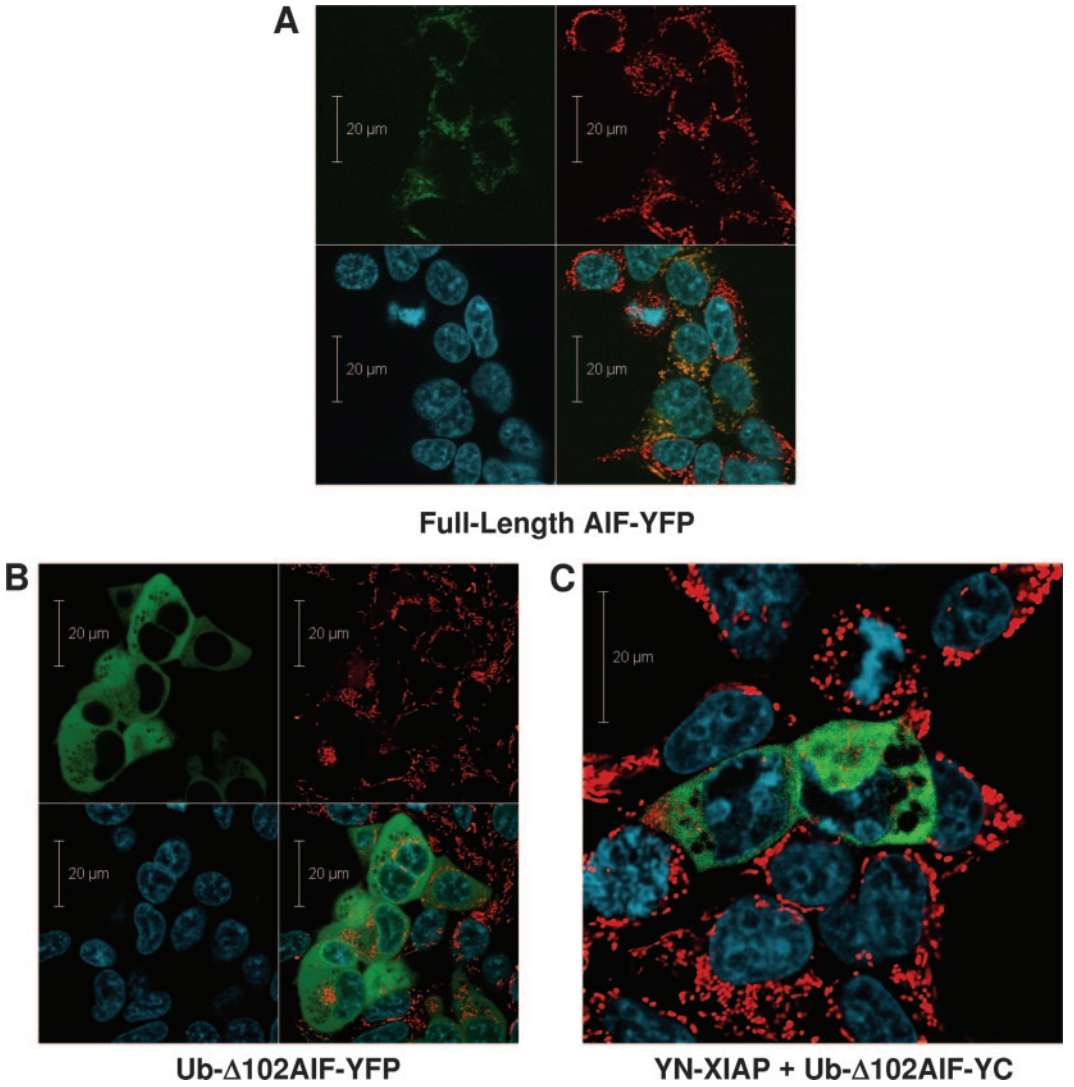

FIG. 4. Fluorescence complementation analysis of the XIAP/AIF interaction. (A and B) Full-length AIF (A) and Ub-Δ102AIF (B) in fusion with YFP at the carboxy terminus (here shown in green) were expressed in HEK 293 cells. Cells were stained with Mitotracker Red (red staining) and Hoechst stain (blue staining). The cellular localization of AIF proteins was then determined by confocal microscopy. (C) BiFC was used to examine the XIAP/AIF interaction. YN-XIAP was coexpressed with Ub-Δ102AIF-YC. The green fluorescence observed is indicative of a cytoplasmic interaction between XIAP and Δ102 AIF. Cells were additionally stained with both Mitotracker Red (red) and Hoechst stain (blue).

Since XIAP must bind a substrate in order to induce its ubiquitination, the data presented above suggest that XIAP and Ub-Δ102AIF interact within cells, despite our inability to coprecipitate these two molecules (Fig. 3A). To test this possibility, the BiFC approach (22) was used as an alternative means to investigate the interaction between XIAP and Ub-Δ102AIF. This method is based on the separation of YFP into amino (YN)- and carboxy (YC)-terminal domains, neither of which is fluorescent when the two are coexpressed in cells. When separately fused to two interacting molecules, these YFP domains may recombine, resulting in cellular fluorescence. Thus, this approach not only allows the detection of protein-protein interactions within a living cell but also identifies the subcellular compartment where the interaction occurs. Our laboratory and others have shown that XIAP resides predominantly in the cytoplasm (4). While native AIF in fusion with the complete YFP polypeptide displayed a clear, punctate, mitochondrial localization (Fig. 4A), Ub-Δ102AIF-YFP exhibited a diffuse, cytoplasmic localization pattern (Fig. 4B). When the BiFC combination of YN-XIAP and Ub-Δ102AIF-YC was examined by confocal microscopy, a strong fluorescent signal localized to the cytoplasm was observed (Fig. 4C). Thus, by using the BiFC approach, which is highly sensitive to lower-affinity protein-protein interactions, binding between XIAP and Ub-Δ102AIF was observed in living cells.

The data presented in Fig. 3 and 4 strongly suggest that XIAP binds and ubiquitinates both the healthy and apoptotic forms of AIF, though binding to the latter is transient, with complex stability decaying quickly as AIF becomes ubiquitinated. Thus, the XIAP variant H467A, which lacks E3 ubiquitin ligase activity, should be able to effectively precipitate

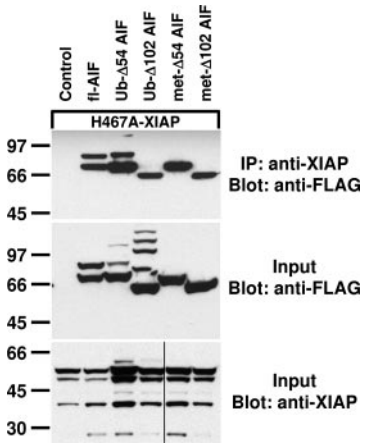

FIG. 5. H467A-XIAP immunoprecipitates all AIF variants. (A) HEK 293 cells were transfected with a plasmid encoding H467A-XIAP along with control, full-length AIF, Ub-Δ54AIF, Ub-Δ102AIF, met-Δ54AIF, or met-Δ102AIF expression plasmids. XIAP was then immunoprecipitated from cell lysates, and the presence of AIF was determined by immunoblot analysis using anti-FLAG (top panel). Equivalent expression of XIAP (bottom panel) and AIF variants (middle panel) was confirmed by immunoblotting input lysates. The black line present in the bottom panel indicates removal of a single empty lane solely for the purpose of clarity. Note that this experiment was carried out in parallel to that shown for WT-XIAP in Fig. 3A so that efficiency of AIF coprecipitation could be compared between the two XIAP variants. Numbers at left are molecular masses in kilodaltons.

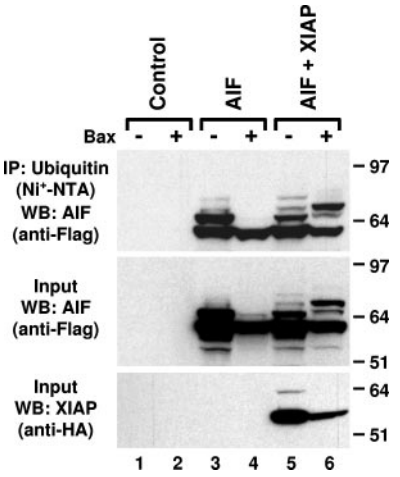

FIG. 6. XIAP ubiquitinates AIF following induction of apoptosis. HEK 293 cells were transfected with His-tagged ubiquitin and either control plasmids (lanes 1 and 2), full-length AIF-FLAG (lanes 3 and 4), or full-length AIF-FLAG and XIAP expression plasmids (lanes 5 and 6), in the absence (lanes 1, 3, and 5) and presence (lanes 2, 4, and 6) of a plasmid encoding Bax. Ubiquitinated material was then precipitated using Ni-NTA beads, and the presence of FLAG-tagged proteins (AIF) in precipitated complexes was detected by immunoblot analysis. Numbers at right are molecular masses in kilodaltons.

Ub-Δ102AIF. As shown in Fig. 5, Ub-Δ102AIF was readily detectable in H467A-XIAP immune complexes, confirming that the lack of detectable Ub-Δ102AIF in WT-XIAP immunoprecipitates is most likely due to XIAP-mediated ubiquitination of Ub-Δ102 AIF, resulting in destabilization of the complex. Furthermore, the remaining forms of AIF appear to precipitate more efficiently with H467A-XIAP than with the WT protein (compare Fig. 5 with Fig. 3A), suggesting that a lack of XIAP-mediated ubiquitination may stabilize these complexes as well.

While the data presented thus far demonstrate that XIAP binds to and ubiquitinates multiple forms of AIF, due to the fact that these data were obtained under postlysis conditions (solubilizing both XIAP and AIF) and/or employed AIF variants that were cytoplasmically localized, a question arises regarding the physiological conditions in which XIAP and AIF interact. This is because in healthy cells XIAP resides predominantly in the cytoplasm, whereas AIF is found in the intermembrane space of the mitochondria; thus, these molecules are normally sequestered in different cellular compartments. To explore this question, a functional approach was employed in which the ubiquitination status of AIF was examined during apoptosis, a condition in which release of AIF from the mitochondria should allow association with XIAP. Bax overexpression in HEK 293 cells induces caspase-dependent cell death and was used as a convenient method of apoptosis induction. Cells were transfected with a plasmid encoding His-tagged ubiquitin along with control, full-length AIF, or full-length AIF and XIAP expression plasmids, in the absence or presence of a plasmid encoding Bax. Ni-NTA beads were then used to precipitate ubiquitinated proteins from cell lysates, and the presence of AIF in precipitated complexes was determined by immunoblot analysis. As shown in Fig. 6, full-length AIF in healthy cells exhibited a moderate amount of ubiquitination in the absence of XIAP, and little to no change was observed following XIAP coexpression (compare lanes 3 and 5), consistent with the results in Fig. 3B. Importantly, the presence of XIAP induced a significantly greater amount of AIF ubiquitination under apoptotic conditions compared to cells lacking the XIAP plasmid (compare lanes 4 and 6), and the electrophoretic mobilities of the detected species were significantly different from the mobilities of those detected in the absence of Bax (compare lanes 5 and 6). These results demonstrate that under apoptotic conditions significant XIAP-mediated ubiquitination of AIF occurs and suggest that XIAP and AIF associate as the cell death cascade proceeds.

In light of the above observation, the effects of XIAP/AIF association on apoptosis were explored further. Our screen isolated AIF by using an XIAP variant incapable of inhibiting caspases, suggesting that the interface of XIAP to which AIF binds may differ from that employed by caspases. Since Smac/DIABLO binds to XIAP in a competitive manner with respect to caspases, this raised the question of whether Smac/DIABLO could also block the XIAP/AIF interaction. XIAP was expressed along with either WT Smac/DIABLO or the Smac/DIABLO mutant Δ1A or A1G, and the ability of Smac/DIABLO to prevent XIAP/AIF association was evaluated by coprecipitation. As shown in Fig. 7, the presence of WT Smac/DIABLO completely prevented the association between XIAP and AIF, whereas the IBM mutants, which fail to bind XIAP, also fail to prevent XIAP/AIF association. These data suggest that the XIAP associations with Smac/DIABLO and AIF are mutually exclusive.

XIAP is a well-characterized caspase inhibitor, a property that allows XIAP to protect cells from a variety of apoptotic stimuli (21). As described above for Fig. 6, in HEK 293 cells

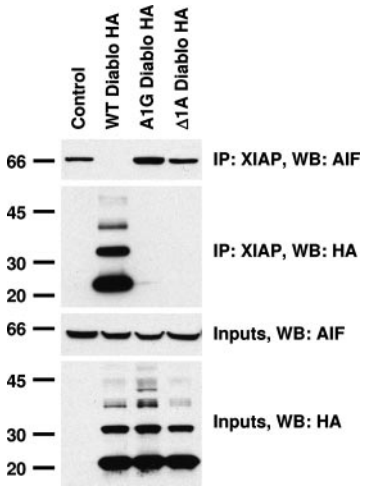

FIG. 7. Smac/DIABLO disrupts the XIAP/AIF interaction. HEK 293 cells were transfected with a plasmid encoding WT-XIAP along with either control, DIABLO-HA, Δ1A-DIABLO-HA, or A1G-DIABLO-HA expression plasmid. Cell lysates were then precipitated with anti-XIAP, and the presence of AIF (anti-AIF, top panel) or Smac/DIABLO (anti-HA, second panel from top) in immune complexes was determined by immunoblot analysis. Equivalent expression of AIF (third panel from top) and Smac/DIABLO (bottom panel) was assessed by immunoblot analysis of input lysates. Numbers at left are molecular masses in kilodaltons.

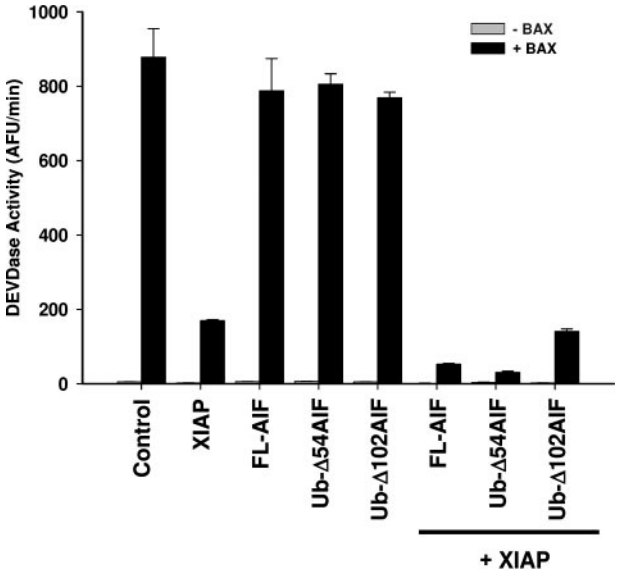

FIG. 8. AIF does not prevent XIAP-mediated caspase inhibition. HEK 293 cells were transfected with the indicated plasmids, cell lysates were prepared, and the activation of caspase 3 was determined by incubation with the fluorogenic caspase 3 substrate DEVD–7-amino-4-trifluoromethyl coumarin.

Bax overexpression effectively induces caspase-dependent death; in this setting XIAP overexpression effectively prevents apoptosis, and this protection can be reversed by coexpression of Smac/DIABLO (60). To determine if AIF, like other XIAP binding proteins, can neutralize XIAP-mediated caspase inhibition, we examined the effects of AIF expression in this model system. As shown in Fig. 8, Bax expression resulted in robust caspase activation, which was significantly reduced by expression of XIAP, as expected. When the three AIF variants (full length, Ub-Δ54, and Ub-Δ102) were expressed alone in the absence and presence of Bax, no noticeable differences were observed in the levels of caspase activity. Importantly, none of the AIF variants were capable of inducing caspase activation when expressed in the absence of cotransfected Bax, consistent with Fig. 4A and B, in which full-length AIF-YFP and Ub-Δ102AIF-YFP exhibited no toxicity. Finally, when coexpressed with XIAP none of the AIF variants were able to prevent XIAP-mediated caspase inhibition. Taken together, these data suggest that the interaction between XIAP and AIF does not alter the caspase-inhibitory properties of XIAP, indicating that AIF does not function as an IAP antagonist, and further raise the possibility that the interaction between XIAP and AIF serves to regulate caspase-independent functions of both proteins.

While the results of Fig. 6 confirm that an interaction occurs between XIAP and AIF following permeabilization of the outer mitochondrial membrane, they do not rule out the possibility that XIAP and AIF may coregulate within cells that are not undergoing apoptosis. The enzymatic and signal-transducing properties of AIF in healthy cells are presently ill defined, with the best-described property being in vitro NADH-oxidase activity (36). Since AIF can affect the oxidative state of cells through this enzymatic function, the ability of AIF to regulate intracellular ROS levels was tested in the absence and presence of XIAP, both under basal conditions and following treatment with the ROS-generating agent antimycin A. HEK 293 cells were transfected with AIF or XIAP expression plasmids either individually or in combination prior to treatment with antimycin A. Cells were then stained with the general-purpose ROS indicator dye CM-H_2DCF-DA, and cellular fluorescence was determined by flow cytometry (Fig. 9). Whereas expression of full-length AIF resulted in a slight increase in both basal and antimycin A-stimulated ROS levels, both AIF truncation variants significantly reduced both basal and stimulated levels of ROS. Interestingly, XIAP was also capable of decreasing ROS, to an extent that exceeded that of all three AIF variants. Importantly, the coexpression of XIAP with each of the AIF variants resulted in a progressive decrease in observed ROS levels (both basal and stimulated), such that the combination of XIAP and AIF reduced ROS levels following antimycin A treatment to those observed in untreated control cells, suggesting that the combined effects of XIAP and AIF on ROS are to reduce overall cellular oxidative stress. This last observation also confirms that XIAP-mediated ubiquitination of AIF does not result in proteasomal degradation, since such an effect would have been expected to reverse the AIF-mediated decrease in ROS following coexpression of XIAP with AIF.

DISCUSSION

XIAP is a multifunctional protein that can regulate numerous intracellular signaling cascades. In order to identify factors that participate with XIAP in regulating both caspase-dependent and -independent pathways, we conducted a biochemical screen and identified AIF as an XIAP-associated protein. The physical association between AIF and XIAP requires the second BIR domain of the XIAP protein, a similar determinant

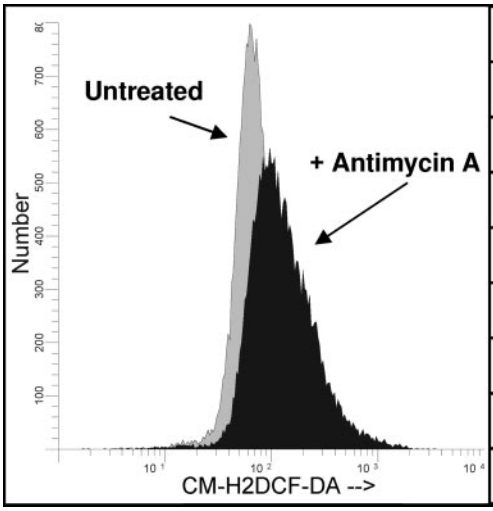

Sample	Untreated	+ Antimycin A
Control	83.37 ± 3.76	152.70 ± 14.0
FL-AIF	102.15 ± 3.04	171.55 ± 7.42
Ub-Δ54-AIF	65.75 ± 2.22	115.90 ± 14.1
Ub-Δ102-AIF	56.41 ± 3.20	100.90 ± 3.96
XIAP	44.72 ± 2.04	80.21 ± 2.84
FL-AIF + XIAP	62.30 ± 3.78	104.01 ± 15.7
Ub-Δ54-AIF + XIAP	37.89 ± 2.28	67.74 ± 3.40
Ub-Δ102-AIF + XIAP	35.62 ± 0.13	60.58 ± 4.74

FIG. 9. Effects of XIAP/AIF expression of ROS formation. HEK 293 cells were transfected with control or XIAP expression plasmids in the absence and presence of either full-length AIF, Ub-Δ54 AIF, or Ub-Δ102 AIF. Cells were then left untreated or treated with antimycin A and stained with the ROS-indicating dye CM-H_2-DCFDA, and cellular ROS levels were determined by flow cytometry. Representative histograms of untreated (gray) and antimycin A-treated (black) cells are shown, and values shown are the average ±1 standard deviation of three replicate measurements.

used by XIAP for interaction with caspases 3 and 7. However, AIF binds the XIAP variant D148A/W310A, a variant lacking caspase-inhibitory properties, suggesting that the nature of the interaction between XIAP and AIF is different from the nature of those between XIAP and the executioner caspases. Interestingly, Smac/DIABLO interferes with the binding of XIAP to AIF, suggesting that there is overlap in the binding epitopes within XIAP employed by these two mitochondrial proteins.

The XIAP/AIF interaction is complex due to the existence of two distinct forms of AIF, as well as to the differing extents of ubiquitination observed for these AIF variants. We show here that the mature form of human AIF in healthy cells lacks the first 54 amino-terminal residues, which is consistent with a previous report describing both healthy and apoptotic forms of rat AIF (41). XIAP binds both forms of AIF, and the extent of binding correlates with AIF ubiquitination status. Indeed, through the E3 ubiquitin ligase activity of its RING domain, XIAP induces the ubiquitination of AIF, and the Δ102 form appears to be a better substrate than the Δ54 form, explaining the failure of Δ102AIF to coprecipitate with WT XIAP. Importantly, the reduced ability of Δ102 to coprecipitate with XIAP is not a consequence of ubiquitination-induced AIF degradation, since AIF levels appear unaffected following ubiquitination by XIAP. Surprisingly, the XIAP variant H467A, which is devoid of E3 ubiquitin ligase activity, binds more robustly to all forms of AIF. We have previously reported that H467A XIAP is a dominant-negative protein with respect to E3 ligase activity (60); thus, the increased coprecipitation of AIF by H467A-XIAP may be due to a general reduction of AIF ubiquitination, resulting in increased affinity for XIAP.

Despite the ability of AIF to bind XIAP, this interaction does not result in an attenuation of the caspase-inhibitory properties of the XIAP protein. Indeed, not only does the coexpression of AIF fail to prevent XIAP from inhibiting Bax-mediated caspase activation and cell death, but a slight improvement to XIAP-mediated protection was observed when AIF was coexpressed. Interestingly, none of the forms of AIF studied, including the presumptively prodeath Δ102 form, were capable of inducing death when expressed alone. This observation is in contrast to previous reports describing the ability of AIF to kill cells with single-agent toxicity (51) and is consistent with more-recent studies suggesting that the death-promoting capacity of AIF is dependent upon prior caspase activation (1, 38).

While AIF was originally discovered as an agent involved in completing the apoptotic cascade (51), a unifying model describing the role of AIF in cell death remains elusive. Indeed, accumulating evidence suggests that the role of AIF in cell death varies tremendously in both a tissue-specific and a stimulus-dependent manner. For example, in neuronal cells AIF plays a key role in the completion of both caspase-dependent and -independent death pathways (10, 11), particularly following ischemia/reperfusion injury or glutamate excitotoxicity (10, 64). Conversely, not only does the loss of AIF in cardiomyocytes fail to prevent ischemia/reperfusion-induced death, but cells lacking AIF are more sensitive to this stimulus (56). In peripheral T cells, AIF is required for the successful completion of activation-induced cell death, but the absence of AIF has no effect on DNA damage-induced apoptosis (49). In light of these observations, our study defining the association between XIAP and AIF takes on new significance, as it suggests that these two molecules may coordinately regulate multiple forms of cell death in a tissue-specific manner.

Though in vitro studies have characterized the NADH-oxidase function of the protein, clear characterization of the enzymatic properties of AIF in a cellular context has not been reported. AIF loss-of-function studies, such as in mice with either natural reduction (28) or tissue-specific targeted deletion (9, 26) of AIF, suggest that AIF functions to preserve mitochondrial function. This may occur by AIF serving as a general-purpose antioxidant, through regulation of the activity and/or expression of complex I of the mitochondrial electron

transport chain or through maintenance of mitochondrial structure by as-yet-unknown mechanisms. We report here that the expression of either Δ54 or Δ102 AIF results in a decrease in the levels of ROS, consistent with a role for AIF as an antioxidant. Interestingly, expression of XIAP also appears to reduce cellular ROS levels, and the simultaneous expression of AIF and XIAP has an additive effect. Whether this is due to the XIAP/AIF interaction or is through the independent function of each protein is unclear. But to our knowledge this is the first report linking XIAP to the regulation of intracellular ROS, suggesting an additional mechanism by which XIAP controls cellular signal transduction.

Since the original description of XIAP as a high-affinity caspase inhibitor, a number of additional properties of XIAP have been described. Indeed, in light of the observation that mice lacking XIAP display no overt defects in apoptosis, it could be argued that the predominant in vivo function of XIAP is to participate in signal transduction cascades distinct from those involving caspases. Our observations here that XIAP is capable of interacting with AIF, that this interaction does not affect caspase inhibition by XIAP, and that both AIF and XIAP can additively reduce intracellular ROS levels support this point of view. As with XIAP, the apparent biological properties of AIF are complex. While originally described as a prodeath molecule capable of both caspase-dependent and -independent apoptotic functions, more-recent evidence points to a prosurvival activity for AIF, predominantly by preserving mitochondrial function and integrity. Experiments reported here show that enforced expression of AIF is not cytotoxic and may be protective since a general decrease in basal ROS levels was observed. The mechanism(s) by which AIF and XIAP regulate cellular oxidative stress, both separately and in combination, remains to be elucidated. However, a role for both proteins in this process highlights their multifaceted roles in controlling intracellular signaling.

We show that XIAP binds to and induces the ubiquitination of both the healthy and apoptotic forms of AIF. The possible consequences of this interaction require more complete definition, but since XIAP-mediated ubiquitination does not result in AIF degradation, they include alteration of AIF enzymatic activity, attenuation of the apoptotic effects of AIF, or alterations in as-yet-undefined properties of the AIF protein. Given the high level of attention cast towards regulators of the cell death cascade for the purposes of therapeutic intervention in human diseases, the data presented here raise the level of importance of understanding the total functions of both XIAP and AIF, as well as the significance of their interaction in vivo.

ACKNOWLEDGMENTS

We are grateful to T. Kerppola for providing BiFC plasmids and to L. Boise and E. Burstein for critical discussions.

This work was supported by the University of Michigan Biomedical Scholars Program (to C.S.D.), grants R01 GM067827 (to C.S.D.) and T32 CA09676 (to R.A.C.) from the National Institutes of Health, and grants W81XWH-04-1-0891 (to C.S.D.) and W81XWH-04-1-0854 (to J.C.W.) from the Department of Defense Prostate Cancer Research Program.

REFERENCES

1. **Arnoult, D., M. Karbowski, and R. J. Youle.** 2003. Caspase inhibition prevents the mitochondrial release of apoptosis-inducing factor. Cell Death Differ. **10:**845–849.
2. **Birkey Reffey, S., J. U. Wurthner, W. T. Parks, A. B. Roberts, and C. S. Duckett.** 2001. X-linked inhibitor of apoptosis protein functions as a cofactor in transforming growth factor-β signaling. J. Biol. Chem. **276:**26542–26549.
3. **Budihardjo, I., H. Oliver, M. Lutter, X. Luo, and X. Wang.** 1999. Biochemical pathways of caspase activation during apoptosis. Annu. Rev. Cell Dev. Biol. **15:**269–290.
4. **Burstein, E., L. Ganesh, R. D. Dick, B. van De Sluis, J. C. Wilkinson, J. Lewis, L. W. J. Klomp, C. Wijmenga, G. J. Brewer, G. J. Nabel, and C. S. Duckett.** 2004. A novel role for XIAP in copper homeostasis through regulation of MURR1. EMBO J. **23:**244–254.
5. **Burstein, E., J. E. Hoberg, A. S. Wilkinson, J. M. Rumble, R. A. Csomos, C. M. Komarck, G. N. Maine, J. C. Wilkinson, M. W. Mayo, and C. S. Duckett.** 2005. COMMD proteins: a novel family of structural and functional homologs of MURR1. J. Biol. Chem. **280:**22222–22232.
6. **Cain, K., D. G. Brown, C. Langlais, and G. M. Cohen.** 1999. Caspase activation involves the formation of the aposome, a large (approximately 700 kDa) caspase-activating complex. J. Biol. Chem. **274:**22686–22692.
7. **Chai, J., C. Du, J. W. Wu, S. Kyin, X. Wang, and Y. Shi.** 2000. Structural and biochemical basis of apoptotic activation by Smac/DIABLO. Nature **406:** 855–862.
8. **Chai, J., E. Shiozaki, S. M. Srinivasula, Q. Wu, P. Dataa, E. S. Alnemri, and Y. Shi.** 2001. Structural basis of caspase-7 inhibition by XIAP. Cell **104:**769–780.
9. **Cheung, E. C., N. Joza, N. A. Steenaart, K. A. McClellan, M. Neuspiel, S. McNamara, J. G. MacLaurin, P. Rippstein, D. S. Park, G. C. Shore, H. M. McBride, J. M. Penninger, and R. S. Slack.** 2006. Dissociating the dual roles of apoptosis-inducing factor in maintaining mitochondrial structure and apoptosis. EMBO J. **25:**4061–4073.
10. **Cheung, E. C., L. Melanson-Drapeau, S. P. Cregan, J. L. Vanderluit, K. L. Ferguson, W. C. McIntosh, D. S. Park, S. A. Bennett, and R. S. Slack.** 2005. Apoptosis-inducing factor is a key factor in neuronal cell death propagated by BAX-dependent and BAX-independent mechanisms. J. Neurosci. **25:** 1324–1334.
11. **Cregan, S. P., A. Fortin, J. G. MacLaurin, S. M. Callaghan, F. Cecconi, S. W. Yu, T. M. Dawson, V. L. Dawson, D. S. Park, G. Kroemer, and R. S. Slack.** 2002. Apoptosis-inducing factor is involved in the regulation of caspase-independent neuronal cell death. J. Cell Biol. **158:**507–517.
12. **Cryns, V., and J. Yuan.** 1998. Proteases to die for. Genes Dev. **12:**1551–1570.
13. **Deveraux, Q. L., and J. C. Reed.** 1999. IAP family proteins—suppressors of apoptosis. Genes Dev. **13:**239–252.
14. **Du, C., M. Fang, Y. Li, L. Li, and X. Wang.** 2000. Smac, a mitochondrial protein that promotes cytochrome *c*-dependent caspase activation by eliminating IAP inhibition. Cell **102:**33–42.
15. **Duckett, C. S., V. E. Nava, R. W. Gedrich, R. J. Clem, J. L. Van Dongen, M. C. Gilfillan, H. Shiels, J. M. Hardwick, and C. B. Thompson.** 1996. A conserved family of cellular genes related to the baculovirus *iap* gene and encoding apoptosis inhibitors. EMBO J. **15:**2685–2694.
16. **Eckelman, B. P., G. S. Salvesen, and F. L. Scott.** 2006. Human inhibitor of apoptosis proteins: why XIAP is the black sheep of the family. EMBO Rep. **7:**988–994.
17. **Hao, Z., G. S. Duncan, C. C. Chang, A. Elia, M. Fang, A. Wakeham, H. Okada, T. Calzascia, Y. Jang, A. You-Ten, W. C. Yeh, P. Ohashi, X. Wang, and T. W. Mak.** 2005. Specific ablation of the apoptotic functions of cytochrome C reveals a differential requirement for cytochrome C and Apaf-1 in apoptosis. Cell **121:**579–591.
18. **Harlin, H., S. B. Reffey, C. S. Duckett, T. Lindsten, and C. B. Thompson.** 2001. Characterization of XIAP-deficient mice. Mol. Cell. Biol. **21:**3604–3608.
19. **Hegde, R., S. M. Srinivasula, Z. Zhang, R. Wassell, R. Mukattash, L. Cilenti, G. DuBois, Y. Lazebnik, A. S. Zervos, T. Fernandes-Alnemri, and E. S. Alnemri.** 2002. Identification of Omi/HtrA2 as a mitochondrial apoptotic serine protease that disrupts IAP-caspase interaction. J. Biol. Chem. **277:** 432–438.
20. **Hofer-Warbinek, R., J. A. Schmid, C. Stehlik, B. R. Binder, J. Lipp, and R. de Martin.** 2000. Activation of NF-κB by XIAP, the X chromosome-linked inhibitor of apoptosis, in endothelial cells involves TAK1. J. Biol. Chem. **275:**22064–22068.
21. **Holcik, M., and R. G. Korneluk.** 2001. XIAP, the guardian angel. Nat. Rev. Mol. Cell Biol. **2:**550–556.
22. **Hu, C. D., Y. Chinenov, and T. K. Kerppola.** 2002. Visualization of interactions among bZIP and Rel family proteins in living cells using bimolecular fluorescence complementation. Mol. Cell **9:**789–798.
23. **Huang, Y., Y. C. Park, R. L. Rich, D. Segal, D. G. Myszka, and H. Wu.** 2001. Structural basis of caspase inhibition by XIAP. Differential roles of the linker versus the BIR domain. Cell **104:**781–790.
24. **Hunter, A. M., D. Kottachchi, J. Lewis, C. S. Duckett, R. G. Korneluk, and P. Liston.** 2003. A novel ubiquitin fusion system bypasses the mitochondria and generates biologically active Smac/DIABLO. J. Biol. Chem. **278:**7494–7499.
25. **Itoh, S., M. Thorikay, M. Kowanetz, A. Moustakas, F. Itoh, C. H. Heldin, and P. ten Dijke.** 2003. Elucidation of Smad requirement in transforming

growth factor-β type I receptor-induced responses. J. Biol. Chem. **278:**3751–3761.

26. **Joza, N., G. Y. Oudit, D. Brown, P. Benit, Z. Kassiri, N. Vahsen, L. Benoit, M. M. Patel, K. Nowikovsky, A. Vassault, P. H. Backx, T. Wada, G. Kroemer, P. Rustin, and J. M. Penninger.** 2005. Muscle-specific loss of apoptosis-inducing factor leads to mitochondrial dysfunction, skeletal muscle atrophy, and dilated cardiomyopathy. Mol. Cell. Biol. **25:**10261–10272.
27. **Kerr, J. F., A. H. Wyllie, and A. R. Currie.** 1972. Apoptosis: a basic biological phenomenon with wide-ranging implications in tissue kinetics. Br. J. Cancer **26:**239–257.
28. **Klein, J. A., C. M. Longo-Guess, M. P. Rossmann, K. L. Seburn, R. E. Hurd, W. N. Frankel, R. T. Bronson, and S. L. Ackerman.** 2002. The harlequin mouse mutation downregulates apoptosis-inducing factor. Nature **419:**367–374.
29. **Levkau, B., K. J. Garton, N. Ferri, K. Kloke, J. R. Nofer, H. A. Baba, E. W. Raines, and G. Breithardt.** 2001. XIAP induces cell-cycle arrest and activates nuclear factor-κB: new survival pathways disabled by caspase-mediated cleavage during apoptosis of human endothelial cells. Circ. Res. **88:**282–290.
30. **Lewis, J., E. Burstein, S. B. Reffey, S. B. Bratton, A. B. Roberts, and C. S. Duckett.** 2004. Uncoupling of the signaling and caspase-inhibitory properties of XIAP. J. Biol. Chem. **279:**9023–9029.
31. **Li, P., D. Nijhawan, I. Budihardjo, S. M. Srinivasula, M. Ahmad, E. S. Alnemri, and X. Wang.** 1997. Cytochrome *c* and dATP-dependent formation of Apaf-1/caspase-9 complex initiates an apoptotic protease cascade. Cell **91:**479–489.
32. **Liston, P., N. Roy, K. Tamai, C. Lefebvre, S. Baird, G. Cherton-Horvat, R. Farahani, M. McLean, J.-E. Ikeda, A. MacKenzie, and R. G. Korneluk.** 1996. Suppression of apoptosis in mammalian cells by NAIP and a related family of IAP genes. Nature **379:**349–353.
33. **Liu, Z., C. Sun, E. T. Olejniczak, R. P. Meadows, S. F. Betz, T. Oost, J. Herrmann, J. C. Wu, and S. W. Fesik.** 2000. Structural basis for binding of Smac/DIABLO to the XIAP BIR3 domain. Nature **408:**1004–1008.
34. **Martins, L. M., I. Iaccarino, T. Tenev, S. Gschmeissner, N. F. Totty, N. R. Lemoine, J. Savopoulos, C. W. Gray, C. L. Creasy, C. Dingwall, and J. Downward.** 2002. The serine protease Omi/HtrA2 regulates apoptosis by binding XIAP through a Reaper-like motif. J. Biol. Chem. **277:**439–444.
35. **Medema, J. P., C. Scaffidi, F. C. Kischkel, A. Shevchenko, M. Mann, P. H. Krammer, and M. E. Peter.** 1997. FLICE is activated by association with the CD95 death-inducing signaling complex (DISC). EMBO J. **16:**2794–2804.
36. **Miramar, M. D., P. Costantini, L. Ravagnan, L. M. Saraiva, D. Haouzi, G. Brothers, J. M. Penninger, M. L. Peleato, G. Kroemer, and S. A. Susin.** 2001. NADH oxidase activity of mitochondrial apoptosis-inducing factor. J. Biol. Chem. **276:**16391–16398.
37. **Mufti, A. R., E. Burstein, R. A. Csomos, P. C. Graf, J. C. Wilkinson, R. D. Dick, M. Challa, J. K. Son, S. B. Bratton, G. L. Su, G. J. Brewer, U. Jakob, and C. S. Duckett.** 2006. XIAP is a copper binding protein deregulated in Wilson's disease and other copper toxicosis disorders. Mol. Cell **21:**775–785.
38. **Munoz-Pinedo, C., A. Guio-Carrion, J. C. Goldstein, P. Fitzgerald, D. D. Newmeyer, and D. R. Green.** 2006. Different mitochondrial intermembrane space proteins are released during apoptosis in a manner that is coordinately initiated but can vary in duration. Proc. Natl. Acad. Sci. USA **103:**11573–11578.
39. **Nagata, S.** 1996. Apoptosis: telling cells their time is up. Curr. Biol. **6:**1241–1243.
40. **Nicholson, D. W.** 1999. Caspase structure, proteolytic substrates, and function during apoptotic cell death. Cell Death Differ. **6:**1028–1042.
41. **Otera, H., S. Ohsakaya, Z. Nagaura, N. Ishihara, and K. Mihara.** 2005. Export of mitochondrial AIF in response to proapoptotic stimuli depends on processing at the intermembrane space. EMBO J. **24:**1375–1386.
42. **Puig, O., F. Caspary, G. Rigaut, B. Rutz, E. Bouveret, E. Bragado-Nilsson, M. Wilm, and B. Seraphin.** 2001. The tandem affinity purification (TAP) method: a general procedure of protein complex purification. Methods **24:**218–229.
43. **Ranger, A. M., J. Zha, H. Harada, S. R. Datta, N. N. Danial, A. P. Gilmore, J. L. Kutok, M. M. Le Beau, M. E. Greenberg, and S. J. Korsmeyer.** 2003. Bad-deficient mice develop diffuse large B cell lymphoma. Proc. Natl. Acad. Sci. USA **100:**9324–9329.
44. **Riedl, S. J., M. Renatus, R. Schwarzenbacher, Q. Zhou, C. Sun, S. W. Fesik, R. C. Liddington, and G. S. Salvesen.** 2001. Structural basis for the inhibition of caspase-3 by XIAP. Cell **104:**791–800.
45. **Sanna, M. G., J. da Silva Correia, O. Ducrey, J. Lee, K. Nomoto, N. Schrantz, Q. L. Deveraux, and R. J. Ulevitch.** 2002. IAP suppression of apoptosis involves distinct mechanisms: the TAK1/JNK1 signaling cascade and caspase inhibition. Mol. Cell. Biol. **22:**1754–1766.
46. **Sanna, M. G., J. Da Silva Correia, Y. Luo, B. Chuang, L. M. Paulson, B. Nguyen, Q. L. Deveraux, and R. J. Ulevitch.** 2002. ILPIP, a novel anti-apoptotic protein that enhances XIAP-mediated activation of JNK1 and protection against apoptosis. J. Biol. Chem. **277:**30454–30462.
47. **Shiozaki, E. N., J. Chai, D. J. Rigotti, S. J. Riedl, P. Li, S. M. Srinivasula, E. S. Alnemri, R. Fairman, and Y. Shi.** 2003. Mechanism of XIAP-mediated inhibition of caspase-9. Mol. Cell **11:**519–527.
48. **Srinivasula, S. M., R. Hegde, A. Saleh, P. Datta, E. Shiozaki, J. Chai, R. A. Lee, P. D. Robbins, T. Fernandes-Alnemri, Y. Shi, and E. S. Alnemri.** 2001. A conserved XIAP-interaction motif in caspase-9 and Smac/DIABLO regulates caspase activity and apoptosis. Nature **410:**112–116.
49. **Srivastava, S., H. Banerjee, A. Chaudhry, A. Khare, A. Sarin, A. George, V. Bal, J. M. Durdik, and S. Rath.** 2007. Apoptosis-inducing factor regulates death in peripheral T cells. J. Immunol. **179:**797–803.
50. **Sun, C., M. Cai, R. P. Meadows, N. Xu, A. H. Gunasekera, J. Herrmann, J. C. Wu, and S. W. Fesik.** 2000. NMR structure and mutagenesis of the third Bir domain of the inhibitor of apoptosis protein XIAP. J. Biol. Chem. **275:**33777–33781.
51. **Susin, S. A., H. K. Lorenzo, N. Zamzami, I. Marzo, B. E. Snow, G. M. Brothers, J. Mangion, E. Jacotot, P. Costantini, M. Loeffler, N. Larochette, D. R. Goodlett, R. Aebersold, D. P. Siderovski, J. M. Penninger, and G. Kroemer.** 1999. Molecular characterization of mitochondrial apoptosis-inducing factor. Nature **397:**441–446.
52. **Thompson, C. B.** 1995. Apoptosis in the pathogenesis and treatment of disease. Science **267:**1456–1462.
53. **Thornberry, N. A., and Y. Lazebnik.** 1998. Caspases: enemies within. Science **281:**1312–1316.
54. **Uren, A., M. Pakusch, C. Hawkins, K. L. Puls, and D. L. Vaux.** 1996. Cloning and expression of apoptosis inhibitory protein homologs that function to inhibit apoptosis and/or bind tumor necrosis factor receptor-associated factors. Proc. Natl. Acad. Sci. USA **93:**4974–4978.
55. **Vahsen, N., C. Cande, J. J. Briere, P. Benit, N. Joza, N. Larochette, P. G. Mastroberardino, M. O. Pequignot, N. Casares, V. Lazar, O. Feraud, N. Debili, S. Wissing, S. Engelhardt, F. Madeo, M. Piacentini, J. M. Penninger, H. Schagger, P. Rustin, and G. Kroemer.** 2004. AIF deficiency compromises oxidative phosphorylation. EMBO J. **23:**4679–4689.
56. **van Empel, V. P., A. T. Bertrand, R. van der Nagel, S. Kostin, P. A. Doevendans, H. J. Crijns, E. de Wit, W. Sluiter, S. L. Ackerman, and L. J. De Windt.** 2005. Downregulation of apoptosis-inducing factor in harlequin mutant mice sensitizes the myocardium to oxidative stress-related cell death and pressure overload-induced decompensation. Circ. Res. **96:**e92–e101.
57. **Vaux, D. L., and J. Silke.** 2005. IAPs, RINGs and ubiquitylation. Nat. Rev. Mol. Cell Biol. **6:**287–297.
58. **Verhagen, A. M., P. G. Ekert, M. Pakusch, J. Silke, L. M. Connolly, G. E. Reid, R. L. Moritz, R. J. Simpson, and D. L. Vaux.** 2000. Identification of DIABLO, a mammalian protein that promotes apoptosis by binding to and antagonizing IAP proteins. Cell **102:**43–53.
59. **Verhagen, A. M., J. Silke, P. G. Ekert, M. Pakusch, H. Kaufmann, L. M. Connolly, C. L. Day, A. Tikoo, R. Burke, C. Wrobel, R. L. Moritz, R. J. Simpson, and D. L. Vaux.** 2002. HtrA2 promotes cell death through its serine protease activity and its ability to antagonise inhibitor of apoptosis proteins. J. Biol. Chem. **277:**445–454.
60. **Wilkinson, J. C., A. S. Wilkinson, F. L. Scott, R. A. Csomos, G. S. Salvesen, and C. S. Duckett.** 2004. Neutralization of Smac/Diablo by IAPs: a caspase-independent mechanism for apoptotic inhibition. J. Biol. Chem. **279:**51091–51099.
61. **Yamaguchi, K., S. Nagai, J. Ninomiya-Tsuji, M. Nishita, K. Tamai, K. Irie, N. Ueno, E. Nishida, H. Shibuya, and K. Matsumoto.** 1999. XIAP, a cellular member of the inhibitor of apoptosis protein family, links the receptors to TAB1-TAK1 in the BMP signaling pathway. EMBO J. **18:**179–187.
62. **Yang, Y., S. Fang, J. P. Jensen, A. M. Weissman, and J. D. Ashwell.** 2000. Ubiquitin protein ligase activity of IAPs and their degradation in proteasomes in response to apoptotic stimuli. Science **288:**874–877.
63. **Ye, H., C. Cande, N. C. Stephanou, S. Jiang, S. Gurbuxani, N. Larochette, E. Daugas, C. Garrido, G. Kroemer, and H. Wu.** 2002. DNA binding is required for the apoptogenic action of apoptosis inducing factor. Nat. Struct. Biol. **9:**680–684.
64. **Yu, S. W., H. Wang, M. F. Poitras, C. Coombs, W. J. Bowers, H. J. Federoff, G. G. Poirier, T. M. Dawson, and V. L. Dawson.** 2002. Mediation of poly-(ADP-ribose) polymerase-1-dependent cell death by apoptosis-inducing factor. Science **297:**259–263.